Applied Physics Letters

RESEARCH ARTICLE | MAY 16 2024

Multiplying vortex beams by diffraction from almost periodic structures: Theory and experiment

Mohsen Samadzadeh ; Saifollah Rasouli ; Davud Hebri ; Sergey A. Ponomarenko

Appl. Phys. Lett. 124, 201107 (2024)
https://doi.org/10.1063/5.0197721

Applied Physics Letters ARTICLE pubs.aip.org/aip/apl

Multiplying vortex beams by diffraction from almost periodic structures: Theory and experiment

Cite as: Appl. Phys. Lett. **124**, 201107 (2024); doi: 10.1063/5.0197721
Submitted: 14 January 2024 · Accepted: 8 May 2024 ·
Published Online: 16 May 2024

Mohsen Samadzadeh,[1] Saifollah Rasouli,[1,2,a)] Davud Hebri,[3] and Sergey A. Ponomarenko[3,4]

AFFILIATIONS

[1]Department of Physics, Institute for Advanced Studies in Basic Sciences (IASBS), Zanjan 45137-66731, Iran
[2]Center for International Scientific Studies and Collaboration (CISSC), Ministry of Science, Research and Technology, Tehran 15875-7788, Iran
[3]Department of Physics and Atmospheric Science, Dalhousie University, Halifax, Nova Scotia B3H 4R2, Canada
[4]Department of Electrical and Computer Engineering, Dalhousie University, Halifax, Nova Scotia B3J 2X4, Canada

[a)]Author to whom correspondence should be addressed: rasouli@iasbs.ac.ir

ABSTRACT

We advance theoretically and verify experimentally a protocol for generating arrays of self-similar light beams with the aid of almost periodic structures (APSs), which we refer to as pure amplitude 2N-gonal APSs. We illustrate our general results by realizing a circular array of exact replicas of a Laguerre–Gaussian source beam and registering good agreement between the theory and experiment. Our work carries promise for optical communications, optical tweezing, multi-particle trapping, screening, and micro-manipulation.

Optical vortices (OVs) are topologically nontrivial light beams carrying the orbital angular momentum.[1,2] They have important applications to optical tweezing, optical communications, quantum information, and condensed matter physics among others.[3–8]

Optical vortex arrays (OVAs) are arrays of OVs that have found applications to cold atom trapping, microfluidic sorting, and photonic crystal engineering.[9,10] OVAs have also attracted a lot of interest in the context of micro-mechanical pump manipulation, orbital angular momentum mode multiplexing, and quantum information processing.[2]

OVAs can be generated by a variety of techniques. One approach is based on the far-field diffraction of a plane wave or a Gaussian beam by a pure phase 2D orthogonal periodic structure with a phase singularity.[6,11] Another method is based on the near-field diffraction of a vortex beam by a pure amplitude 2D orthogonal periodic structure.[12–14] Diffraction from a phase mask, often encoded onto a liquid-crystal spatial light modulator (SLM), has been employed to generate arrays of vortex beams in various configurations.[15–22] In principle, phase holograms,[23–27] Dammann gratings,[28] direct shaping with axicon[29] or spiral phase arrays,[30,31] or combinations thereof can be used to generate vortex arrays (lattices). In addition, the generation of optical vortex arrays by multiplexing metasurface design is introduced in Ref. 32. All these methods, in principle, enable great flexibility and a wide selection of periodic vortex arrangements. Yet, the majority of OVA generating techniques suffer from multiple drawbacks, including low-efficiency, complexity, cost, or lack of flexibility and scalability.

In this Letter, we propose a general protocol to generate arrays of any self-similar beams with the help of almost periodic structures (APSs). We implement our protocol to realize an annular array of Laguerre–Gaussian (LG) beams, which carry optical vortices, by employing APSs with the spatial spectra composed of impulses at the center and the corners of a regular 2N-sided polygon. We demonstrate that our method can produce versatile optical vortex arrays of variable topological charges, sizes, and field patterns. We stress that our approach works for any shape-invariant (self-similar) beams on free space propagation, and it is complementary to a recently advanced random beam array generation protocol[9] relying on optical coherence lattices.[10,33,34]

We note that by employing an LG beam instead of a Gaussian as in our previous work (Ref. 35), we can enable the angular rotation of trapped particles around the axis of each LG beam. It follows that we can, in principle, simultaneously rotate a set of trapped particles around the array axis and the particle axes (spinning), as well as around the individual array element axes. Thus, a set of spinning particles will orbit along small circles with the radii equal to the widths of the generated LG beams, with the beam axes being equally spaced on a larger circle. At the same time, the particles will orbit around the center of a large array circle.

According to the general theory of diffraction,[36,37] the transmittance function of an APS can be expressed in a generic vector form as

$$t_{\mathrm{APS}}(\mathbf{r}) = \sum_{n=0}^{\infty} t_n e^{i\mathbf{k_n}\cdot\mathbf{r}}, \tag{1}$$

where $\mathbf{r} = (x, y) = (r\cos\varphi, r\sin\varphi)$ is the position vector in transverse plane, $\mathbf{k_n}$ represents the wavevector of a plane wave associated with the nth harmonic Fourier component of the APS transmittance function, and t_n is a Fourier coefficient. The power P_n of the nth diffraction order past the structure is related to the power P_{in} of the incident light beam as[11]

$$\frac{P_n}{P_{\mathrm{in}}} = |t_n|^2. \tag{2}$$

Summing over n on both sides of Eq. (2) and taking into account energy conservation yields

$$\frac{P_{\mathrm{tr}}}{P_{\mathrm{in}}} = \sum_{n=0}^{\infty} |t_n|^2, \tag{3}$$

where $P_{\mathrm{tr}} = \sum_{n=0}^{\infty} P_n$ is a total transmitted power. It follows at once from Eqs. (2) and (3) that

$$\frac{P_n}{P_{\mathrm{tr}}} = \frac{|t_n|^2}{\sum_{n=0}^{\infty} |t_n|^2}, \tag{4}$$

and the ratio of the transmitted power within the nth diffraction order to the total transmitted power is completely determined by the set $\{t_n\}$.

As an example of APSs, we consider a pure amplitude octagonal APS described in Appendix A of Ref. 37 and in Ref. 35. This APS has impulses at the center and vertices of an octagon in the spectral domain. By the same token, we can create a generalized pure amplitude APS with impulses at the center and vertices of any even-sided regular polygon (denoted by $2N$) in the spectral domain. Henceforth, we refer to this structure as a pure amplitude $2N$-gonal APS; its transmission function reads

$$t_{2N}(\mathbf{r}) = \frac{1}{2} + \frac{1}{2N}\sum_{n=1}^{N} \cos(\mathbf{k_n}\cdot\mathbf{r}). \tag{5}$$

Here, $\mathbf{k_n} = (2\pi\nu\cos\theta_n, 2\pi\nu\sin\theta_n)$, where $\theta_n = \pi(n-1)/N$ and ν is a fundamental (spatial) frequency of the structure. Although the structure defined by Eq. (5) is not generally periodic, we can establish a characteristic length, defined as $\Lambda = 1/\nu$, which serves as a fundamental period of the structure. To facilitate comparison with the general form of APSs, Eq. (1), we can rewrite Eq. (5) as follows:

$$t_{2\mathrm{N}}(\mathbf{r}) = \frac{1}{2} + \frac{1}{4N}\sum_{n=1}^{2N} e^{i\mathbf{k}_n\cdot\mathbf{r}}, \tag{6}$$

where we used $\mathbf{k}_{N+m} = -\mathbf{k}_m$ for $m = 1, 2, \ldots, N$ as a result of $\theta_{N+m} = \theta_m + \pi$. On comparing Eqs. (6) and (1), we infer that $t_0 = 1/2$, $t_n = (4N)^{-1}$ for $1 \le n \le 2N$, and $t_n = 0$ for $n > 2N$. The top row of Fig. 1 shows the transmittance functions of several pure amplitude 2N-gonal APSs. The bottom row displays spatial spectra (Fourier transforms) of the transmittance functions of the same APSs, which have $2N+1$ impulses each. These impulses include a zero-order one at the origin, $\mathbf{k} = 0$, and $2N$ others that are arranged along the circumference of a circle around the origin in the reciprocal (Fourier) space. The characteristic length of the structure is $\Lambda = \nu^{-1} = 10\,\mathrm{mm}$. To enhance visibility of the spots, we employ a logarithmic color scale.

It follows from Eq. (3) that $P_{\mathrm{tr}}/P_{\mathrm{in}} = (2N+1)/8N$. In Fig. 2, we exhibit a ratio of the transmitted to incident power for several pure amplitude 2N-gonal APS in the left column. It is evident that as N increases, the transmitted power decreases and approaches 25% of the incident power. We denote the power of the zero diffraction order at the origin in Fig. 1 as P_0, and the total power of the impulses on the circumference of the circle as P_{circle}. We can infer from Eqs. (3)–(5) the fractions that the zero-order impulse power and that due to the other diffracted orders make of the total transmitted power: $P_0/P_{\mathrm{tr}} = 2N/(2N+1)$

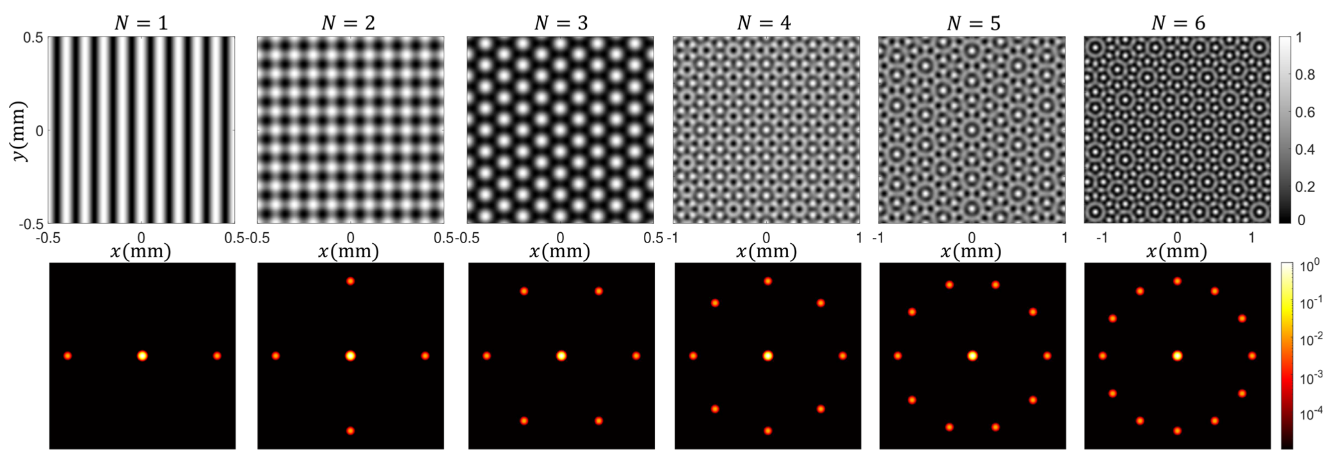

FIG. 1. Top row: transmittance functions of several pure amplitude 2N-gonal APSs with $\Lambda = 0.1$ mm and varied N. Bottom row: the corresponding spatial spectra in a logarithmic color scale.

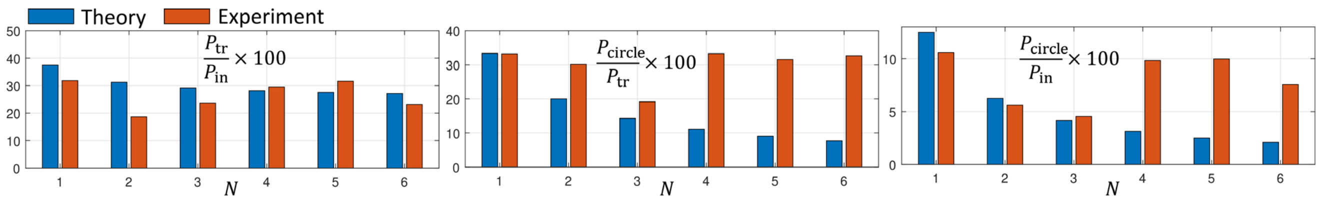

FIG. 2. Power transmittance of pure amplitude 2N-gonal APSs in terms of N (left column). Total power fraction of the impulses distributed over the circle circumference, P_{circle}, relative to the transmitted power (middle column) and relative to the incident power (right column).

and $P_{\text{circle}}/P_{\text{tr}} = 1/(2N+1)$. Moreover, the fractions of the incident power of the DC impulse and the other impulses are $P_0/P_{\text{in}} = 1/4$ and $P_{\text{circle}}/P_{\text{in}} = (8N)^{-1}$, respectively. We present the power fractions of the impulses along the circle relative to the transmitted and incident powers, respectively, in the middle and right columns of Fig. 2.

Let us now consider an arbitrary optical beam transmitted by an APS structure located in the source plane $z = 0$. The optical field immediately behind the structure reads

$$\Psi(\mathbf{r}, 0) = u(\mathbf{r}, 0) t_{\text{APS}}(\mathbf{r}), \tag{7}$$

where $u(\mathbf{r}, 0)$ is a complex amplitude of the incident beam. The light field has spatial coherence and illuminates almost the entire surface of the structure. On subsequent free space propagation, the field in any transverse plane $z = const \geq 0$ is related to that just past the APS by a Fresnel transform as[38]

$$\Psi(\mathbf{r}, z) = \left(\frac{k}{2\pi i z}\right) \int d\mathbf{r}' \Psi(\mathbf{r}', 0) e^{ik|\mathbf{r}-\mathbf{r}'|^2/2z}, \tag{8}$$

where $k = 2\pi/\lambda$ is the wave number of the carrier frequency of the beam. On combining Eqs. (1), (7), and (8) and regrouping the exponential terms, we arrive at the expression[35]

$$\Psi(\mathbf{r}, z) = e^{ikr^2/2z} \sum_{n=0}^{\infty} t_n e^{-ikr_n^2/2z} u(\mathbf{r_n}, z), \tag{9}$$

where $\mathbf{r_n} = \mathbf{r} - \mathbf{k_n} z/k$ in which $\mathbf{k_n} z/k$ is a position vector of the center of the nth diffraction order so that $\mathbf{r_n}$ can be regarded as the position vector in the coordinates transformed to the center of the nth diffraction order. We can also write $\mathbf{r_n} = (r_n \cos\varphi_n, r_n \sin\varphi_n)$ by considering $r_n = |\mathbf{r_n}| = \sqrt{x_n^2 + y_n^2}$ and $\varphi_n = \tan^{-1}\left(\frac{y_n}{x_n}\right)$ as polar coordinates around the center of nth diffraction order.

If the source generates shape-invariant beams, Eq. (9) describes a superposition of shifted, scaled replicas of the source field weighed with quadratic phase factors. It follows that when an APS is illuminated by a self-similar optical beam, the diffraction orders can, under certain circumstances, precisely replicate the incident beam. In other words, over sufficiently long distances from the APS, where distinct diffraction orders separate, we can realize an array of nearly perfect replicas of the incident beam. Moreover, the shape of the array can be engineered with the APSs as well. Similarly, we can achieve the same array in a scaled version at the focal plane of a lens by placing the lens after the structure.

As an example, we consider a pure amplitude 2N-gonal APS having components with sinusoidal profiles presented by Eq. (6). In this case, on substituting $t_0 = 1/2$, $t_n = (4N)^{-1}$ for $1 \leq n \leq 2N$, and $t_n = 0$ otherwise into Eq. (9), we obtain in polar coordinates (r, θ) the expression

$$\Psi(\mathbf{r}, z) = \frac{1}{2} u(\mathbf{r}, z) + \frac{e^{-2i\pi z/z_T}}{4N} \sum_{n=1}^{2N} e^{2i\pi\nu r \cos(\theta-\theta_n)} u(\mathbf{r_n}, z), \tag{10}$$

where $z_T = 2\Lambda^2/\lambda$ denotes the Talbot distance of the structure. We now specify to the incident LG beams. In polar coordinates, the field of an LG beam at $z = 0$ can be expressed as[39]

$$u(\mathbf{r}, 0) \propto \left(\frac{r}{w_0}\right)^{|l|} e^{-\frac{r^2}{w_0^2} + il\varphi} L_p^{|l|}\left(\frac{2r^2}{w_0^2}\right), \tag{11}$$

where l and w_0 indicate the topological charge and width of the beam at the waist, respectively. Further, $L_p^{|l|}$ denotes an associated Laguerre polynomial, and p is the radial index of the beam. Upon propagation over the distance z in free space, the field is well known to remain shape-invariant such that[39]

$$u(\mathbf{r}, z) \propto g_p^l(z) e^{i\left(\frac{kr^2}{2q(z)} + l\varphi\right)} \left(\frac{r}{w(z)}\right)^{|l|} L_p^{|l|}\left(\frac{2r^2}{w^2(z)}\right), \tag{12}$$

where $g_p^l(z)$, $q(z)$, and $w(z)$ have been defined in Eqs. (11)–(14) of Ref. 40. Suppose an APS with a transmittance indicated by Eq. (6) is illuminated by the LG beam. We can then determine the diffracted light field at the distance z from the APS with the aid of Eqs. (10) and (12).

We now discuss our experimental realization of the LG array. In Fig. 3, we sketch our experimental setup for the implementation of LG beam arrays of variables l and p. We use different amplitude fork gratings with almost binary profiles to generate different LG beams. We illuminate the fork grating of given charge and radial index with a Gaussian beam produced by a neodymium-doped yttrium aluminum

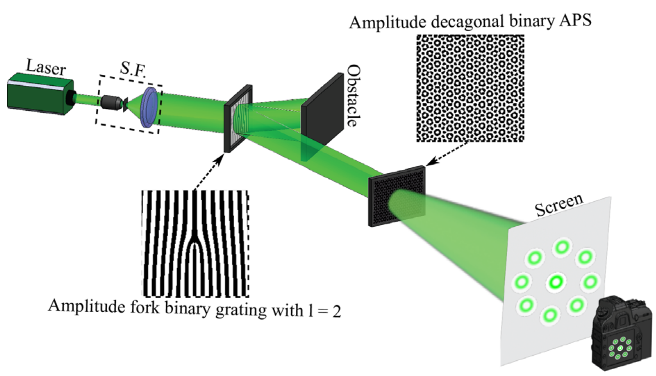

FIG. 3. Experimental setup for generating and multiplying LG beams using different amplitude fork gratings and pure amplitude 2 N-gonal APSs. S.F. stands for a spatial filter.

garnet (ND:YAG) diode-pumped laser of wavelength $\lambda = 532$ nm. The left inset in the figure panels shows a typical amplitude fork grating pattern. The generated LG beam then passes through a pure amplitude 2N-gonal APS. The right inset in the figure panels shows a typical pure amplitude 2N-gonal APS. We employ a camera (Nikon D7200) to capture the diffracted pattern with precision and record it directly onto the camera sensor. To obtain a high-resolution and aberration-free image of the diffraction pattern, we remove the imaging lens of the camera and record the pattern directly onto the camera sensor.

In Figs. 4 and 5 (Multimedia views), we observe good agreement between our theoretical predictions and experimental patterns (red and green, respectively). As expected, the realized arrays contain $2N + 1$ LG modes, comprising a more powerful central mode and $2N$ modes, all with the same field structure, arranged in a circular pattern around the origin of the center (see also the background Visualizations 1–8 “Multimedia view”). In Fig. 2, we compare the actual and theoretically predicted power ratios of the diffraction orders. Notably, in the third column of Fig. 2, for N = 4, we experimentally measured the ratio of P_{circle} to P_{in} as 10%. This implies that the power share for each multiplied vortex beam amounts to 1.25% of the incident beam power. Remarkably, this power share exceeds the theoretically expected value. Additionally, it significantly surpasses what would be achieved using an SLM instead of an APS.

We encounter an intriguing phenomenon: the side orders carry more power than initially expected. This unexpected behavior may be attributed to the non-sinusoidal nature of the transmittance profiles within the structures. The theoretical predictions were based on the assumption that the APSs exhibit sinusoidal profiles. However, upon closer examination of the printed patterns, we observe that they tend to resemble binary-like transmission patterns. This discrepancy arises due to the inherent nature of the fabricated structures. Specifically, the binary-like transmission patterns lead to a more balanced power distribution between the zeroth and first diffraction orders. Unlike the idealized sinusoidal profiles, which tend to favor the zeroth order, our printed patterns feature a fairly even power distribution among these orders. Consequently, the measured amplitudes of the surrounding spots are significantly higher than anticipated.

In conclusion, we have developed a general method for generating arrays of shape-invariant optical vortex beams with the aid of diffraction gratings. We have implemented the method to realize a set of vortex carrying LG beams on a circular array employing pure amplitude 2N-gonal APSs. In our approach, we eliminate the need for SLMs both during vortex beam generation and multiplication. Instead, we employ different amplitude fork gratings to create the impinging vortex beams, which subsequently diffracts from pure amplitude APSs. Notably, the fork and APS structures can be conveniently printed on sheet plastic plates, making our approach straightforward, cost-efficient, and user-friendly. While SLMs offer precise control over optical beam properties, their diffraction efficiency remains a challenge due to the inherent characteristics of their 2D periodic structure. These methods are often expensive due to complex construction requirements. Moreover, working with SLMs can be intricate, necessitating

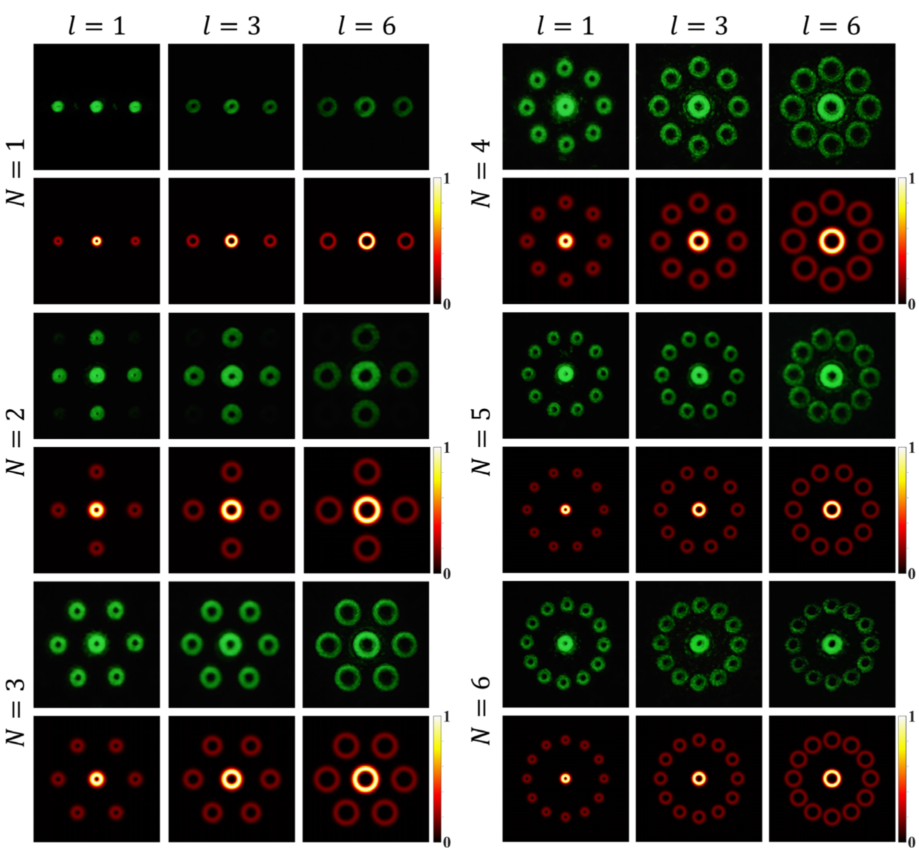

FIG. 4. Theoretical and experimental results for generated LG beam arrays with $p = 0$ and variable l by pure amplitude 2N-gonal APSs with adjustable N. The odd rows show experimental results, while the even ones exhibit our theoretical predictions. Multimedia available online.

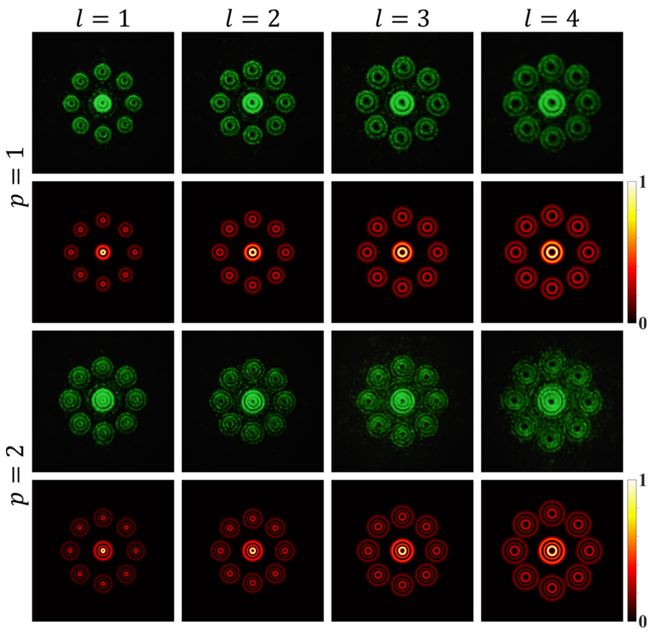

FIG. 5. Multiplication of LG beams of variable p and l with the aid of a pure amplitude 2N-gonal APS having $N = 4$. Odd rows correspond to our experimental results, while even ones show our theoretical predictions. Multimedia available online.

computer systems for operation. Indeed, consider the intensity efficiency of an SLM illuminated by a plane wave. Even without shaping the amplitude and phase of an optical field, the 2D periodic structure results in each diffraction order receiving less than 1% of the incident beam power. If we, in addition, impose a phase/amplitude onto the field with the SLM, the transmitted power redistributes among desired secondary diffracted orders. Unfortunately, this re-sharing leads to a very low intensity in the desired diffraction orders. Researchers then face a formidable challenge of enhancing the power share in the desired diffraction order, especially if the SLM is employed to realize multi-particle traps. Our method offers a practical alternative, bypassing SLM complexities and providing an accessible solution for vortex beam manipulation. Our technique has potential for a number of applications, including optical communications, optical tweezing, multi-particle trapping, screening, and micro-manipulation. The application of the presented protocol to multiple particle trapping that simultaneously imparts spinning and two distinct orbital rotations to the particles, and the investigation of near-field diffraction of LG beams from APSs are in progress. We illustrate some preliminary results in Fig. 5 background Visualizations 7 and 8, where the diffracted light is simultaneously focused by a thin lens.

S.R. acknowledges support from the ICTP through the Associates Program (No. 2018-2023). This work is partially funded by Centre for International Scientific Studies and Collaboration (CISSC) of Iran under Project No. 4020667 and Iran National Science Foundation (INSF) under Project No. 4020609. D.H. acknowledges the Izaak Walton Killam Postdoctoral Fellowship, and SAP acknowledges support from NSERC (No. RGPIN-2018-05497).

This study was supported by the Institute for Advanced Studies in Basic Sciences (No. G2023IASBS12632), Center for International Scientific Studies and Collaboration (CISSC) of Iran (No. 4020667), Iran National Science Foundation (No. 4020609), and Natural Sciences & Engineering Research Council (NSERC) of Canada (No. RGPIN-2018-05497).

AUTHOR DECLARATIONS

Conflict of Interest

The authors have no conflicts to disclose.

Author Contributions

Mohsen Samadzadeh: Data curation (equal); Methodology (equal); Visualization (equal). **Saifollah Rasouli:** Conceptualization (lead); Data curation (equal); Formal analysis (equal); Funding acquisition (lead); Investigation (equal); Methodology (equal); Project administration (lead); Resources (lead); Supervision (lead); Validation (lead); Visualization (equal); Writing – original draft (equal); Writing – review & editing (equal). **Davud Hebri:** Conceptualization (equal); Formal analysis (equal); Investigation (equal); Methodology (equal); Validation (equal); Visualization (equal); Writing – original draft (equal); Writing – review & editing (equal). **Sergey A. Ponomarenko:** Formal analysis (equal); Investigation (equal); Methodology (equal); Validation (equal); Writing – original draft (equal); Writing – review & editing (equal).

DATA AVAILABILITY

The data that support the findings of this study are available from the corresponding author upon reasonable request.

REFERENCES

[1]Y. Shen, X. Wang, Z. Xie, C. Min, X. Fu, Q. Liu, M. Gong, and X. Yuan, "Optical vortices 30 years on: OAM manipulation from topological charge to multiple singularities," Light **8**, 1–29 (2019).

[2]X. Wang, Z. Nie, Y. Liang, J. Wang, T. Li, and B. Jia, "Recent advances on optical vortex generation," Nanophotonics **7**, 1533–1556 (2018).

[3]M. Padgett and R. Bowman, "Tweezers with a twist," Nat. Photonics **5**, 343–348 (2011).

[4]H. He, N. Heckenberg, and H. Rubinsztein-Dunlop, "Optical particle trapping with higher-order doughnut beams produced using high efficiency computer generated holograms," J. Mod. Opt. **42**, 217–223 (1995).

[5]J. Wang, "Advances in communications using optical vortices," Photonics Res. **4**, B14–B28 (2016).

[6]G. Gibson, J. Courtial, M. J. Padgett, M. Vasnetsov, V. Pas'ko, S. M. Barnett, and S. Franke-Arnold, "Free-space information transfer using light beams carrying orbital angular momentum," Opt. Express **12**, 5448–5456 (2004).

[7]X.-L. Wang, X.-D. Cai, Z.-E. Su, M.-C. Chen, D. Wu, L. Li, N.-L. Liu, C.-Y. Lu, and J.-W. Pan, "Quantum teleportation of multiple degrees of freedom of a single photon," Nature **518**, 516–519 (2015).

[8]G. F. Q. Rosen, P. I. Tamborenea, and T. Kuhn, "Interplay between optical vortices and condensed matter," Rev. Mod. Phys. **94**, 035003 (2022).

[9]C. Liang, X. Zhu, C. Mi, X. Peng, F. Wang, Y. Cai, and S. A. Ponomarenko, "High-quality partially coherent Bessel beam array generation," Opt. Lett. **43**, 3188–3191 (2018).

[10]C. Liang, X. Liu, Z. Xu, F. Wang, W. Wen, S. A. Ponomarenko, Y. Cai, and P. Ma, "Perfect optical coherence lattices," Appl. Phys. Lett. **119**, 131109 (2021).

[11]A. M. Khazaei, D. Hebri, and S. Rasouli, "Theory and generation of heterogeneous 2D arrays of optical vortices by using 2D fork-shaped gratings:

Topological charge and power sharing management," Opt. Express **31**, 16361–16379 (2023).
[12]B. Knyazev, O. Kameshkov, N. Vinokurov, V. Cherkassky, Y. Choporova, and V. Pavelyev, "Quasi-Talbot effect with vortex beams and formation of vortex beamlet arrays," Opt. Express **26**, 14174–14185 (2018).
[13]S. Rasouli and D. Hebri, "Theory of diffraction of vortex beams from 2D orthogonal periodic structures and Talbot self-healing under vortex beam illumination," J. Opt. Soc. Am. A **36**, 800–808 (2019).
[14]D. Hebri and S. Rasouli, "Theoretical study on the diffraction-based generation of a 2d orthogonal lattice of optical beams: Physical bases and application for a vortex beam multiplication," J. Opt. Soc. Am. A **39**, 1694–1711 (2022).
[15]X. Li, H. Ma, H. Zhang, Y. Tai, H. Li, M. Tang, J. Wang, J. Tang, and Y. Cai, "Close-packed optical vortex lattices with controllable structures," Opt. Express **26**, 22965–22975 (2018).
[16]A. Kapoor, M. Kumar, P. Senthilkumaran, and J. Joseph, "Optical vortex array in spatially varying lattice," Opt. Commun. **365**, 99–102 (2016).
[17]H. Luo, S. Sang, Z. Xiao, P. Li, F. Wen, Y. Gu, and Z. Wu, "Generation and Talbot effect of optical vortex lattices with high orbital angular momenta," Adv. Quantum Technol. **6**, 2300203 (2023).
[18]M. Bock, S. Das, and R. Grunwald, "Programmable ultrashort-pulsed flying images," Opt. Express **17**, 7465–7478 (2009).
[19]R. Grunwald, T. Elsaesser, and M. Bock, "Spatio-temporal coherence mapping of few-cycle vortex pulses," Sci. Rep. **4**, 7148 (2014).
[20]G.-X. Wei, L.-L. Lu, and C.-S. Guo, "Generation of optical vortex array based on the fractional Talbot effect," Opt. Commun. **282**, 2665–2669 (2009).
[21]L. A. Romero and F. M. Dickey, "Theory of optimal beam splitting by phase gratings. I. One-dimensional gratings," J. Opt. Soc. Am. A **24**, 2280–2295 (2007).
[22]C.-S. Guo, Y. Zhang, Y.-J. Han, J.-P. Ding, and H.-T. Wang, "Generation of optical vortices with arbitrary shape and array via helical phase spatial filtering," Opt. Commun. **259**, 449–454 (2006).
[23]Z. Zhong, W. Tang, H. Yuan, and B. Zhang, "Oam holography for generation and combination of arbitrary structural light array," Opt. Laser Technol. **169**, 110081 (2024).
[24]Y. Lu, B. Jiang, S. Lü, Y. Liu, S. Li, Z. Cao, and X. Qi, "Arrays of Gaussian vortex, Bessel and Airy beams by computer-generated hologram," Opt. Commun. **363**, 85–90 (2016).
[25]D. Wang, L. Jin, C. Rosales-Guzmán, and W. Gao, "Generating arbitrary arrays of circular airy Gaussian vortex beams with a single digital hologram," Appl. Phys. B **127**, 1–5 (2021).
[26]Y. Tang, W. Perrie, J. Schille, U. Loeschner, Q. Li, D. Liu, S. P. Edwardson, A. Forbes, and G. Dearden, "High-quality vector vortex arrays by holographic and geometric phase control," J. Phys. D **53**, 465101 (2020).
[27]G. Wang, X. Kang, X. Sun, Z. Li, Y. Li, K. Chen, N. Zhang, X. Gao, and S. Zhuang, "Generation of perfect optical vortex arrays by an optical pen," Opt. Express **30**, 31959–31970 (2022).
[28]H. Dammann and K. Görtler, "High-efficiency in-line multiple imaging by means of multiple phase holograms," Opt. Commun. **3**, 312–315 (1971).
[29]M. Bock, A. Treffer, and R. Grunwald, "Nondiffracting self-imaging of ultrashort wavepackets," Opt. Lett. **42**, 2374–2377 (2017).
[30]M. Liebmann, A. Treffer, M. Bock, T. Seiler, J. Jahns, T. Elsaesser, and R. Grunwald, "Self-imaging of tailored vortex pulse arrays and spectral Gouy rotation echoes," Opt. Lett. **44**, 1047–1050 (2019).
[31]C. Chen, Y. Fang, C. Jang, W. Chen, H.-C. Lin, and H. Liang, "Systematically investigating the structural variety of crystalline and kaleidoscopic vortex lattices by using laser beam arrays," Appl. Sci. **11**, 8018 (2021).
[32]H. Gao, Y. Li, L. Chen, J. Jin, M. Pu, X. Li, P. Gao, C. Wang, X. Luo, and M. Hong, "Quasi-Talbot effect of orbital angular momentum beams for generation of optical vortex arrays by multiplexing metasurface design," Nanoscale **10**, 666–671 (2018).
[33]L. Ma and S. A. Ponomarenko, "Optical coherence gratings and lattices," Opt. Lett. **39**, 6656–6659 (2014).
[34]Y. Chen, S. A. Ponomarenko, and Y. Cai, "Experimental generation of optical coherence lattices," Appl. Phys. Lett. **109**, 061107 (2016).
[35]P. Yazdani Moghadam, S. Rasouli, F. Hajizadeh, and D. Hebri, "Three-dimensional optical multiple trapping using pure amplitude octagonal almost periodic structures," Opt. Express **31**, 43490–43505 (2023).
[36]I. Amidror, *The Theory of the Moiré Phenomenon: Volume I: Periodic Layers* (Springer, 2009).
[37]D. Hebri and S. Rasouli, "Diffraction from two-dimensional orthogonal non-separable periodic structures: Talbot distance dependence on the number theoretic properties of the structures," J. Opt. Soc. Am. A **36**, 253–263 (2019).
[38]J. W. Goodman, *Introduction to Fourier Optics* (Roberts and Company Publishers, 2005).
[39]A. E. Siegman, *Lasers* (University Science Books, 1986).
[40]S. Rasouli, P. Amiri, and D. Hebri, "Transformation of Laguerre-Gaussian beams into 1D array of Hermite-Gaussian modes under the Talbot effect," Opt. Express **31**, 20683–20695 (2023).